AE-314
UDC 621.039.519
621.039.526

AE-314

Activation Doppler Measurements on U238 and U235 in Some Fast Reactor Spectra

L. I. Tirén and I. Gustafsson

AKTIEBOLAGET ATOMENERGI
STOCKHOLM, SWEDEN 1968

ACTIVATION DOPPLER MEASUREMENTS ON U238 AND U235 IN SOME FAST REACTOR SPECTRA

L I Tirén and I Gustafsson

ABSTRACT

Measurements of the Doppler effect in U238 capture and U235 fission have been made by means of the activation technique in three different neutron spectra in the fast critical assembly FR0. The experiments involved the irradiation of thin uranium metal foils or oxide disks, which were heated in a small oven located at the core centre. The measurements on U238 were extended to 1780 ^{o}K and on U235 to 1470 ^{o}K. A core region surrounding the oven was homogenized in order to facilitate the interpretation of results. The reaction rates in the uranium samples were detected by gamma counting.

The experimental method was checked with regard to systematic errors by irradiations in a thermal spectrum.

The data obtained for U238 capture were corrected for the effect of neutron collisions in the oven wall, and were extrapolated to zero sample thickness. In the softest spectrum (core 5) a Doppler effect (relative increase in capture rate) of 0.260 ± 0.018 was obtained on heating from 343 to 1780 ^{o}K, and in the hardest spectrum (core 3) the corresponding value was 0.030 ± 0.003.

An appreciable Doppler effect in U235 fission was obtained only in the softest spectrum, in which the measured increase in fission rate on heating from 320 to 1470 ^{o}K was 0.007 ± 0.003.

Printed and distributed in March 1968.

LIST OF CONTENTS

1. INTRODUCTION

Measurements of the Doppler effect in fast critical assemblies are usually made by means of a reactivity method, heating either a relatively small sample - pile oscillator method - or a large part of the core medium - Doppler loop experiment. A high precision has been obtained in several recent experiments of this kind, and particularly the pile oscillator method has been refined. The reactivity signal, however, will generally be affected by thermal expansion effects which tend to obscure the Doppler effect to some extent. Experience has shown that this problem can be serious with regard to measurements on fissile samples (U235, Pu239) in which the Doppler effect is very small. It is also believed that the effects of thermal expansion would be enhanced in a small system having a high neutron leakage component such as the FR0 critical assembly, because a scale-down of equipment would entail thermal insulation problems.

The activation Doppler experiment, in which the induced activities in a hot and a cold sample are compared after irradiation, represents an alternative method. Here the mentioned kind of difficulty does not occur; furthermore, the experimental equipment involved is relatively inexpensive. These circumstances led us to adopt the activation method for Doppler studies in the FR0 assembly. The theoretical background of the method was discussed by Storrer et al. [1] in 1963 and was first applied in the MSCA facility by Pflasterer et al. in 1964. A detailed paper has been given by Pflasterer in Ref. [2]. It has later been applied in ZPR III by Davey and Amundson [3], in ZEBRA by M. J. Smith et al. [4] and in the blanket of the BR-1 reactor by Orlov et al. [5]. Activation Doppler measurements have also been made by Perkin et al. [6], using a Sb-Be photo neutron source, and by Seufert and Stegemann, who, by means of a slowing-down time spectrometer, obtained energy dependent Doppler effect data [7].

It should be pointed out that the information gained from the activations is somewhat different from that obtained by reactivity measurements. In the former case very small heated samples (foils) can be used.

This is an experimental advantage, because the amount of spectrum distorting materials can be kept small. The spectrum in the hot sample is primarily determined by the cold reactor core material, i.e. a resonance integral of the form

$$I(T) = \int \sigma_c (T) \frac{\Sigma_p}{\Sigma_t(T_o)} \, dE$$

is involved. (T is the hot sample temperature and T_o is the cold reactor core temperature.) In the reactivity measurement, on the other hand, the sample is necessarily comparatively large and sets up its own spectrum, i.e. the Doppler effect is due mainly to the temperature dependence of a resonance integral of the form

$$I(T) = \int \sigma_c (T) \frac{\Sigma_p}{\Sigma_t(T)} \, dE$$

In the case of a fissile sample (U235, Pu239) another difference is that in the activation measurement only the Doppler effect on the fission cross section is measured (fission product gammas being detected), whereas in the reactivity measurement the signal gives the net effect of a positive fission and a negative capture component.

For these reasons it is thought that the two methods complement each other.

In the present work measurements were made on U238 and U235 in FR0 assemblies with different neutron spectra. The temperature range was extended to 1470 ^{o}K for U235 and 1780 ^{o}K for U238, thus bringing the measurements to temperatures characteristic of power reactor fuels. In this paper the experimental methods and results will be presented; a comparison with theoretical results will be given in a second paper. The experiments have previously been described, in part, at the I.A.E.A. Symposium on Fast Reactor Physics and Related Safety Problems, Oct. 30 - Nov. 3, 1967 [8]. A description of the FR0 reactor is given elsewhere [9].

2. SCOPE OF PRESENT WORK

Measurements of the Doppler effect have been made in cores 3, 5 and 8 of FR0, having core centre neutron spectra plotted in Figure 1. The softest of these (core 5) is broadly similar to that of a steam cooled fast power reactor, and the hardest one (core 3) is not too different from that of a voided Na-cooled reactor. All three cores are fuelled with uranium metal, enriched to 20 % U235. They are diluted with graphite to 29.2 % by volume. In addition cores 8 and 5 contain 1.9 and 7.5 % of polythene, $(CH_2)_n$, respectively. The atomic compositions and critical masses are given in Table 1. All cores are surrounded by a thick copper reflector.

Table 1

Core No.	Atomic densities, 10^{22} at/cm^3						Crit. mass kg U235
	U235	U238	C12	H1	SS*	Al 27	
3	0.568	2.234	2.47	-	0.55	-	111.1
5	0.498	1.963	2.77	0.604	0.55	-	78.7
8	0.498	1.963	2.55	0.151	0.55	0.34	112**

* Fe: 0.41, Ni: 0.048, Cr: 0.096x10^{22} at/cm^3

** Uncorrected value

The measured quantities were the changes in the U238 capture and the U235 fission rates with temperature. A thin sample containing either of these materials was heated in a small oven located in a homogenized region at the core centre. A similar sample was located outside the oven for monitoring purposes. The reaction rates were measured by detecting the induced γ-activity using NaI crystals. The irradiation arrangements, counting techniques and measurement errors are discussed in Sections 5, 6 and 7 respectively.

Two different ovens were used, one for the heating of uranium metal foils to 900 °K and one for UO_2 disks up to 1800 °K. The ovens are described in Section 3. In the case of U235 the temperature was limited to 1500 °K, because of the problem of leakage of volatile fission products from the plate surface at higher temperatures. Since gross fission product γ-ray counting was employed, leakage of fission products during irradiation would introduce a systematic error.

The method was checked by irradiations in a thermal spectrum, in which there is no Doppler effect. These experiments confirmed that no significant systematic errors were made. This is further dealt with in Section 7.2.

In the fast spectrum irradiations the effects of several shortcomings in the experimental set-up were investigated. The effects are represented by the following titles:

- Heterogeneity of core composition
- Effect of collisions in the oven wall
- Finite sample thickness.

3. CONSTRUCTION OF OVENS

Figures 2 and 3 show the ovens used for heating to 900 °K and 1800 °K, respectively. The former is heated by a thermocoax resistance wire, which is embedded in a steel structure. The dissipated heat is transferred by conduction to a foil holder made of aluminium. The foil holder and heating element are surrounded by a thin heat shield. The oven wall is made of aluminium 0.5 mm thick. The hot joints of chromel-alumel thermocouples are located in the foil holder on each side of the foil. This arrangement makes it possible to determine the foil temperature to ± 10 °K or better. A power of about 8 W is needed to heat the foil to 900 °K. The uranium metal foil is 13.5 or 15.0 mm in diameter and 0.050 or 0.062 mm thick. The foil has a central 2 mm diameter hole which facilitates an accurate alignment in the oven and in the sample holder for counting.

The high temperature oven, shown in Figure 3, employs a tantalum wire for heating. The wire is wound around pins of alumina which are supported by molybdenum wires passing through the alumina pins and welded to a thin Mo structure. The samples consist of 0.3 mm thick UO_2 disks, 12 x 12 mm^2 in area. The UO_2 disk is located between the two sections of the heating wire and passes into grooves in the alumina pins. In this oven the heat is transferred to the sample by radiation. Molybdenum shields surround the wire and sample. Another two thin reflectors are inserted between the heater and the wall of the oven. In initial measurements a steel casing was used, which had longitudinal fins for cooling. After overall reliability had been established it was replaced by an aluminium casing in order to reduce wall effects. Thermocouples are located in the structure supporting the heating element. The temperature of the UO_2 disk is calibrated out-of-pile and can be determined with an accuracy of ± 25 ^{o}K at a temperature of 1800 ^{o}K. A power of about 70 W is needed to heat the sample to 1800 ^{o}K.

In both ovens the casing (diameter 2.9 cm, length 8.0 cm) is pushed over a sealing rubber gasket onto the end wall flange. The heating element and supporting structure are fastened to the end wall which contains inlets for power, thermocouples and the evacuation tube. These feed lines and those used for cooling gas pass through the core and top reflector of the reactor and occupy a space 7.1 x 14.2 mm^2 in section. The evacuation system provides a vacuum of $\leq 10^{-3}$ mm Hg. This is sufficient to prevent oxidation of the samples and loss of heat.

During irradiation in the reactor, a flow of nitrogen is maintained around the oven in order to limit the surface temperature to less than 370 ^{o}K in a run at 1800 ^{o}K sample temperature. The nitrogen also provides an inert atmosphere, which should be advantageous in the case of a rupture of the oven.

Since the heating wire material, tantalum, has strong resonances, wires of less neutron absorbing materials (Mo, Zircalloy II) were tried. Only the tantalum wire, however, exhibits an acceptable life. The other materials become extremely brittle due to grain growth.

Therefore tantalum wires of different section areas (0.03 and 0.07 mm^2) were used; no effect of interaction with this material was observed.

4. URANIUM METAL AND OXIDE SAMPLES

The uranium metal foils were punched from 0.05 or 0.062 mm sheets. The loose oxide layer (U_3O_8) was removed by dipping the foils in nitric acid. The thin UO_2 layer then formed was quite stable and deteriorated only very slowly.

The UO_2 disks were made from micronized UO_2 powder with a carbon content less than 70 ppm. On sintering at 2100 °K the resulting samples had densities of 9.5-10.5 g/cm^3 which was sufficient for a practically complete retention of fission products at temperatures up to 1470 °K. The sintered disks were ground to the correct dimensions (12 x 12 x 0.3 mm). In order to study variations in the Doppler effect with uranium thickness, some of the UO_2 was mixed with alumina (50 % by weight) or molybdenum (75 % by weight). The mixtures were sintered in the same way as the pure UO_2 disks. The UO_2-containing samples could be heated to 1800 °K in about 30 min. without any risk of fracture.

The material used for U238 (n,γ) measurements was depleted to 0.2 or 0.4 % U235, and that for U235 (n,f) was enriched to 93 %.

5. IRRADIATION ARRANGEMENTS

Figure 4 shows the positioning of the oven in the central fuel element. The surrounding uranium, graphite and polythene plates were arranged in a heterogeneous pattern. The typical uranium and graphite plate thickness was 3.55 or 7.10 mm. The heterogeneity of composition introduced a source of systematic uncertainty. After initial measurements in core 5 the core region around the oven was therefore made more homogeneous. The uranium and graphite plates in the homogenized zone were 0.6 mm thick and the polythene plates 0.1 mm thick. The lattice average heterogeneity effect associated with a certain fuel plate thickness can be estimated by using a Dancoff corrected σ_b-value for the resonance absorber [10], based on equivalence theory, as shown in Appendix I. The following values were obtained in a typical case (U238(n,γ), core 5)[1]:

---

1) The potential scattering cross section of U238 is not included.

σ_b(homogeneous) = 19.2 b

σ_b(fuel = 0.06 cm) = 18.4 b

σ_b(fuel = 0.71 cm) = 15.4 b

These estimates can be used in calculations to give the effect of heterogeneity, although local effects cannot be obtained, of course. The irradiation arrangement with the homogenized zone is shown in Figure 5. The zone had an average thickness of about 2.8 cm, corresponding to 1.6-1.7 scattering mean free paths in the resonance region. Most of the neutrons (~ 80 %) absorbed by the sample therefore made their last collision in the homogenized zone.

Each experiment included two irradiations, one hot and one cold. In the counting of gamma activities following each irradiation the activation ratio of the in-oven sample and the monitoring sample (located on the end wall of the oven, cf Figure 3) was determined. Denoting this ratio by R, e.g.:

$$R = \frac{\text{Specific U238(n,}\gamma\text{)-activity in sample inside oven}}{\text{Specific U238(n,}\gamma\text{)-activity in sample outside oven}}$$

one obtains for the Doppler effect, D

$$D = \frac{R(\text{hot})}{R(\text{cold})} - 1 \qquad (1)$$

As a check of reproducibility copper foils were fastened on the end wall and on the casing at the level of the uranium sample inside the oven. In initial experiments at 870 ^{o}K copper foils were also placed adjacent to the uranium sample inside the oven for flux monitoring. But the activation rate in copper proved to be temperature-dependent, due to Doppler broadening. Later, in the case of U238, the U238(n,f) reaction in the Doppler samples was used as a complementary flux monitor. This could be done because the contribution from the U235(n,f) reaction is less than 10 %, and the Doppler effect for the latter re-

action is very small (cf Section 8). It was not found, however, that normalization to the appropriate Cu(n,γ) or U238(n,f) activities significantly improved the reproducibility of D (cf Section 8). Nevertheless, the copper foils were included in most measurements, because it was thought that a large error in positioning of the oven might be reflected in the copper activation ratio. Most of the irradiations were made at a reactor power of 40 Watts and lasted for 20 min.

6. GAMMA ACTIVITY COUNTING

A layout of the γ-counting station is shown in Figure 6. It is assembled from commercial units mainly. The detectors consist of two NaI crystals which are 3 in. in diameter and 1 in. thick. Most of the electronics is transistorized and very stable. The equipment is installed in a temperature-stabilized room. An automatic sample changer is included in the arrangement, its operation being controlled by the SAMSES unit, which, after each completed counting interval, causes the relevant information to be punched onto the output tape. The data are processed by a code which performs all the necessary corrections and calculates the activation ratios together with a statistical analysis of the data. The errors in determining the activation ratio of two samples by means of this equipment were examined. Since only relative measurements were involved, the electronics' drift could be effectively eliminated, and it was found that the lack of reproducibility in the count rate ratio not due to the statistics of radioactive decay was less than 0.03 %. Furthermore, pairs of foils which were believed to be identical, except for an accurately determined small difference in weight, were compared. The corrected count rate ratios of such pairs (U235, U238 and Cu samples), excluding diluted UO_2 samples (cf below), deviated in no case by more than 0.10 % from the expected values. A detailed account of counting techniques is given elsewhere [11].

In the case of the U238(n,γ) reaction the 2.3 days decay of Np239 was detected in a ~ 40 keV window around the main 106 keV peak. An activity contribution from fission products of 5 to 10 per cent

was present in this energy interval, however. The correction was obtained in complementary measurements by means of a γ-γ coincidence detector station [12] in which the fission product contribution is suppressed to (1.0±0.5) % in the considered applications. This manner of counting was used only in a few runs on each core since the low coincidence count rate necessitates a very long counting period (2 days) to yield an accuracy of about 0.3 %. Coincidence counting was also necessary for the UO_2-Mo disks in which the Tc99 deexcitation γ at 140 keV otherwise contaminates the Np239 activity.

In the case of the U235(n,f) and U238(n,f) reactions integral counting of fission product gamma was employed. The count rate N(t) was fitted to a function of the type

$$N(t) = \frac{A}{t+\theta} \quad \text{or} \quad N(t) = A \cdot t^{-\alpha}$$

over evaluation intervals during which N(t) did not change more than, say, a factor of two.

When using the U238(n,f) reaction for flux monitoring the strong Np239 activity must be prevented from disturbing the fission product counting. This was done by choosing a discrimination level corresponding to 660 keV, above which energy there is no Np239 γ-activity [12].

7. ANALYSIS OF ERRORS

7.1 Random errors

Estimates of random errors were obtained by repeating the measurements. The estimated standard error in a single measurement of R(hot)/R(cold) is ± 0.3 %. The errors in counting and effective sample weights correspond to an uncertainty of about 0.15 %. This includes the small error due to differences in sample thickness giving different γ-ray self-absorption effects, which was corrected for using empirical absorption coefficients (deduced from irradiations in a thermal spectrum). A large part of the total random error must therefore be attributed to other sources.

Intercalibration of samples was obtained by means of irradiation on a rotating drum in a thermal spectrum, hence differences in resonance self-shielding due to small variations in sample thickness could not be discovered. In the case of the UO_2-Al_2O_3 and UO_2-Mo disks segregation of the UO_2 and diluent yields a similar effect. In fact, initial measurements using the latter type of sample yielded large discrepancies which were attributed to segregation. This difficulty was overcome by using the same disks in the hot and cold runs, which had then to be separated in time by about 1 month for the γ-activity to decay. In complementary measurements the same procedure was also used with the non-diluted samples (U metal and pure UO_2), but not to such an extent as to prove that a reduced standard error was achieved. It should be pointed out that, because of the strong resonance shielding in the fast cores, the specific activation rate does not depend strongly on sample thickness. It is estimated from calculations that a thickness difference of 1 %, which is typical of the samples used, yields an activation difference of less than 0.1 %.

The major part of the random error, i.e. about 0.2 %, is therefore attributed to a lack of reproducibility of the samples in the oven and on the casing and of the oven in the reactor. There may also be a contribution from slight variations in the positioning of the innermost heat reflector. It is believed that an improvement of reproducibility would be possible using a more rigid structure in and around the oven, but such an arrangement would be weighty and therefore accompanied by a distortion of the neutron spectrum, giving a much more serious systematic effect

When coincidence counting was employed the count rate ratios were generally determined with ± 0.3 % accuracy. The corresponding estimated standard error in R(hot)/R(cold) is then increased to ± 0.5 %.

7.2 Systematic effects

Thermal irradiations

In order to discover systematic errors a series of irradiations was carried out in a thermal neutron spectrum in which there is no Doppler effect. In these measurements a possible effect due to the axial

thermal expansion or lateral movement of the sample holder inside the oven should be discovered. The particular effect looked for in the case of U235 was leakage ("boiloff") of fission products from the heated sample. Information about diffusion properties of fission products in uranium metal [13] and oxide [14] indicates that no appreciable leakage would occur at the considered temperatures, but experimental proof was necessary.

Two identical ovens (one hot, one cold) were irradiated adjacent to one another in a horizontal channel of the thermal column of the R2-0 research reactor. Thin foils of copper or tungsten were used for flux monitoring. The irradiation and analysing procedures were similar to those of the fast spectrum runs. The following results were obtained:

Irradiation	$\frac{R(hot)}{R(cold)} - 1$
U238 oxide, 1370-1670 °K	-0.001 ± 0.002*
U235 metal, 870 °K	-0.0010 ± 0.0014*
U235 metal, 1070 °K	-0.013 ± 0.003
U235 oxide, 1470 °K	-0.001 ± 0.003*

* Errors based on observed variations in repeated measurements.

The measurements on U238 confirm, within a limit of error of 0.2 %, that there is no effect of heating other than the Doppler effect.

In the case of U235 there is a very large flux depression inside the sample which depends on the uranium density and thus is affected by thermal expansion. The U235 metal foils were therefore interspaced with copper monitoring foils to make up a sandwich of two 0.062 mm U-foils and three 0.05 mm Cu-foils (plus fission product stopping foils). It was then possible to account for the change in flux depression. The UO_2 disks (0.3 mm) were too thick to allow a similar arrangement in the 1470° runs. The value of R(hot)/R(cold) - 1 actually measured in this case was 0.008 ± 0.003. According to a theoretical esti-

mate, derived in Appendix II, the reduced flux depression in the heated sample yields a value of 0.009. The result quoted in the preceding table, -0.001 ± 0.003, is the difference of these two numbers. Consequently, there is no significant systematic effect in the first and last U235 measurements. In the case of U-metal heated to 1070 °K, on the other hand, there is a considerable reduction in activity on heating, which is attributed to the leakage of fission products.

Effect of self-absorption of gamma activity in the samples

As a result of resonance shielding in the thin samples the Np239 (or fission product) activity is depressed at the centre of the sample. Doppler broadening of the resonances will make the depression somewhat weaker at high temperature. Now in the presence of γ-ray self-absorption in the samples, as suggested by Pflasterer [2], this could lead to a relative underestimate of the activity from the hot sample and thus to a systematic underestimate of the Doppler effect. A simple calculation, however, indicates that the effect is entirely negligible for realistic values of the relevant parameters. Experimental confirmation was obtained from measurements with sandwiches consisting of four U238 metal foils. The Doppler effects derived from measurements on the inner pair and the outer pair of foils were in good agreement.

7.3 Temperature measurements

The temperatures of the hot and cold samples were measured with thermocouples as briefly described in Section 3. These measurements were straightforward and the uncertainties involved are less significant than those of the gamma activity measurements.

The location of the "cold" sample on the end wall of the oven was chosen because it could be accurately reproduced. The temperature in this position was in the range 308-345 °K in the various hot runs. This should be remembered when comparing the results with theory, since cross section data are usually given at 300 °K.

In the results to follow quoted temperature values below 900 °K have an estimated maximum uncertainty of ± 10 °K and above 900°K ± 25 °K.

7.4 Homogeneity of environment

In the measurements reported by Davey and Amundson [3] the measured Doppler effect in U238 samples was found to be sensitive to the orientation of the fuel and diluent plates in the core region. Although the region with thin plates around the oven in the present experiments should be almost homogeneous - as indicated by the σ_b-values given in Section 5 - experimental confirmation of this assumption was judged to be essential. Heterogeneity effects were studied in the softest spectrum - core 5 - by comparing results from the first set of measurements with 3.55-7.10 mm uranium plates (Figure 4) with those of the later runs with 0.6 mm plates. In the latter case an additional test was made by surrounding the oven on all sides with 0.6 or 7.1 mm uranium plates. In the normal arrangement there is a uranium plate on one side of the oven and a graphite or polythene plate on the opposite side. The following results were obtained for the Doppler effect in U238:

Temperature range	Plate arrangement in core	D (uncorrected)
308- 873 °K	0.6 mm U plates	0.118 ± 0.003
	3.55/7.10 mm U plates	0.106 ± 0.005
343-1780 °K	Normal arrangement	0.185 ± 0.003
	0.6 mm U plates all sides	0.185 ± 0.003
	7.1 mm U plates all sides	0.158 ± 0.003

These values show clearly that the effect of heterogeneity in the normal "homogeneous" arrangement is insignificant in the softest neutron spectrum. The same conclusion will hold in the harder spectra also, in which fine structure is less pronounced.

8. RESULTS AND DISCUSSION

The immediate experimental results are sets of values of the Doppler effect, D, given as a function of the wall thickness of the oven (Figure 7), sample thickness (Figure 8) or temperaure (Figures 9 and

10). In order to obtain quantities which can be more easily compared with theoretical results, however, the extrapolation of the measured values to zero sample thickness and zero wall thickness of the oven will be considered.

8.1 Extrapolation to zero wall thickness and zero sample thickness

Figure 7 illustrates the effect of variations in the wall thickness of the casing of the oven. The effect was studied by inserting steel plates between the oven and the surrounding core region. The abscissa is the effective collision probability, P_W, of the wall. Values of P_W were computed using the Wigner approximation

$$P_W = \frac{2\Sigma t}{1+2\Sigma t} \tag{2}$$

(t = effective wall thickness; Σ = macroscopic cross section of wall material).

A more accurate expression, derived by Reynolds [16], yields slightly ($\sim$ 10 %) lower values of P_W in the interval $0 < 2\Sigma t < 0.5$ but the simpler formula, Eq. (2), was preferred in view of the uncertainties involved. The estimated error in P_W is shown by the horizontal bars in Figure 7. It is composed of a constant part arising from the contribution to the reaction rate by neutrons passing through the end walls and supporting structure inside the oven and a variable part, taken as $\pm\ 0.1 \cdot P_W$, which reflects the error in using Eq. (2) and which dominates at large values of P_W.

In the first presentation of the results [8] values of D for zero wall thickness were estimated by linear extrapolation. This procedure, however, is not generally adequate, as shown by the following analysis.

The effective resonance capture integral of a U238 sample (or fission integral of a U235 sample) can be written as follows:

$$I_1(T) = (P_W + \bar{\ell}\Sigma_{p1}) \cdot I_{10}(T) + (1 - P_W) \cdot I_{11}(T) \tag{3}$$

$$I_{10}(T) = \int \sigma_{c1}(T) \frac{1}{1 + \bar{\ell}\Sigma_{t1}(T)}\, dE \tag{4}$$

$$I_{11}(T) = \int \sigma_{c1}(T) \frac{1}{1 + \bar{\ell}\Sigma_{t1}(T)} \cdot \frac{\Sigma_{p3}}{\Sigma_{t3}(T_o)}\, dE \tag{5}$$

These formulae were obtained by simple rearrangement of the expressions due to Reynolds [16]. The notation is:

P_W = Probability that a neutron leaving the foil makes its next collision in the oven wall

$\bar{\ell}$ = mean chord length of sample

σ_{cl} = microscopic resonance cross section (capture, fission) of sample material

Σ_{pi} = macroscopic scattering cross section in region i

Σ_{ti} = macroscopic total cross section in region i

T = sample temperature

T_o = reactor temperature (constant)

i = 1 denotes the sample

i = 3 denotes the surrounding core region.

The first term on the right-hand side of Eq. (3) gives the contribution from neutrons which suffered their last collision in the sample or in the oven wall. With $P_W = 1$ this term equals the effective resonance integral of the sample in a purely moderating medium. The moderating medium is here the oven wall. It is therefore intuitively reasonable that the weight of this integral is reduced by a factor $(P_W + \bar{\ell}\Sigma_{p1}) / (1 + \bar{\ell}\Sigma_{p1})$. The second term is the contribution from neutrons which made their last collision in the homogeneous fuel; the factor $\Sigma_{p3} / \Sigma_{t3}$ in I_{11} can be regarded as a Dancoff factor, giving the shielding effect of the resonance absorber present in the fuel.

Eq. (3) is now used to derive an expression for the measured quantity D in terms of the temperature dependence of I_{10} and I_{11}. Denote

$$\frac{I_{11}(T)}{I_{11}(T_o)} - 1 = D_x(\sigma_b)$$

$$\frac{I_{10}(T)}{I_{10}(T_o)} - 1 = D_s(\sigma_b)$$

$$\frac{I_{10}(T_o)}{I_{11}(T_o)} = f(\sigma_b)$$

$$\sigma_b = \frac{1}{N_U} \cdot \left(\frac{1}{\bar{\ell}} + \Sigma\right)$$

σ_b is the equivalent background cross section and is used instead of $\bar{\ell}$ in order to correlate measurements on uranium metal and oxide samples (including UO_2-Al_2O_3 and UO_2-Mo). N_U is the uranium atomic density and Σ is the total cross section of the other isotopes in the sample (Al, Mo, O). For simplicity the temperature dependence of D_x and D_s is not shown explicitly in the above notation.

From Eq. (3) one now obtains

$$1 + D = \frac{R(hot)}{R(cold)} = \frac{I_1(T)}{I_1(T_o)} = \frac{(P_W + \bar{\ell}\Sigma_{p1})I_{10}(T) + (1 - P_W)I_{11}(T)}{(P_W + \bar{\ell}\Sigma_{p1})I_{10}(T_o) + (1 - P_W)I_{11}(T_o)}$$

which can be rewritten as follows:

$$D = \frac{f \cdot (P_W + \bar{\ell}\Sigma_{p1}) \cdot D_s + (1 - P_W) \cdot D_x}{f \cdot (P_W + \bar{\ell}\Sigma_{p1}) + 1 - P_W} \tag{6}$$

or

$$D_x = D + \frac{f \cdot (P_W + \bar{\ell}\Sigma_{p1})\,(D - D_s)}{1 - P_W} \tag{7}$$

The value of D obtained when $P_W \to 0$ and $\sigma_b \to \infty$ ($\bar{\ell} \to 0$) is $D_x(\sigma_b = \infty)$, which will be denoted D_x^∞. It is the Doppler increment of I_{11} given by Eq. (5) with $\bar{\ell} = 0$:

$$I_{11}(\bar{\ell} = 0) = \int \sigma_{c1}(T) \frac{\Sigma_{p3}}{\Sigma_{t3}(T_o)} dE \tag{8}$$

This resonance integral is more tractable to calculation than the general expression for I_{11} at finite sample thickness. D_x^∞ is therefore the quantity to be deduced from the experiments. The procedure adoped for this pur-

pose was the following. First, values of D_x at different σ_b were determined from the measured data by use of Eq. (7). Then D_x^∞ was obtained by extrapolation.

As regards the first step it is noted that I_{10} and $I_{11}(T_o)$ can be calculated by standard methods, the latter by partial fraction expansion of the integrand [17]. Hence the quantity f can be readily computed. The same is true for D_s, the Doppler effect associated with neutrons which made their last collision in the oven wall or in the sample. The curves shown in Figure 7 are plots of D using Eq. (6), in which D_s and f were theoretical estimates and D_x was obtained by least squares fits to the measured points. Eq. (7) indicates that, when the factor $(P_W + \bar{\ell}\Sigma_p)$ is small, only rough estimates of f and D_s are required to obtain an accurate value of D_x. On the other hand, the correction increases on decreasing sample thickness. This is explained by the fact that f assumes large values for thin samples, particularly in soft neutron spectra, while D_s tends to zero in the limit $\bar{\ell} = 0$.

Table 2 gives the fitted values of D_x for U238 in the different cores. The calculated values of D_s and f-1 ($f \geq 1$, cf Eq. (4) and (5)) were conservatively assumed to be uncertain to ± 50 %. The corresponding inaccuracy in D_x was 2-6 % in the different cases. It is included in the error margins quoted in the table together with the uncertainties due to errors in P_W and the experimental D-values. A large part of the error is common to all values of D_x in a given temperture range and core.

Table 2:

Core No.	Temperature range	σ_b, barns	$D_x(\sigma_b)$ for U238
5	343 - 1780 °K	750	0.226 ± 0.013
		2000	0.247 ± 0.014
		3200	0.253 ± 0.017
	308 - 873 °K	550	0.120 ± 0.007
		2200	0.143 ± 0.009
8	345 - 1750 °K	750	0.085 ± 0.005
		2000	0.093 ± 0.005
3	325 - 1780 °K	750	0.026 ± 0.002

Next, the extrapolation of D_x to zero sample thickness ($\sigma_b = \infty$) will be dealt with. For the thin samples considered, resonance self-shielding is very weak compared with the shielding caused by the uranium in the surrounding fuel region. The dependence of I_{11} and D_x on sample thickness is therefore assumed to be weak enough to permit a linear extrapolation to $\bar{\ell} = 0$ i.e. a linear extrapolation in $\frac{1}{\sigma_b}$. Investigations of the dependence of D_x on σ_b were made on U238 in cores 5 and 8. In all cases the data could be fitted to the relation

$$D_x(\sigma_b) = D_x^{\infty} \left(1 - \frac{105 \pm 20}{\sigma_b}\right) \qquad (9)$$

in the region $\sigma_b > 500$ barns.

The values of D_x^{∞} obtained by extrapolation are given in Table 3 below. The results, which will be discussed further in the following paragraph, can be used for a comparison with theoretical calculations.

The measured data and the resulting values of D_x are plotted in Figure 8 as a function of sample thickness (g/cm^2) and equivalent background cross section. The error margins on D_x are not shown in the figure. By inserting Eq. (9) with the estimated value of D_x^{∞} into Eq. (6) a formula for D as a function of $\bar{\ell}$ and P_W is obtained. The dashed curves drawn in conjunction with the measured points were constructed according to this formula. While a linear extrapolation to $\bar{\ell} = 0$ is reasonable when the oven wall is very thin ($P_W \ll 1$) it may yield false results for thicker oven walls, particularly in a soft neutron spectrum. The slope of the curves near zero sample thickness is due to the simultaneous decrease in D_s and increase in f.

It is concluded that the extrapolations for oven wall and sample size must be made with caution in soft neutron spectra, in which the non-shielded resonance integral I_{10} is large, but the shielded integral I_{11} may be small. In this situation neutrons which have collided in the oven wall receive a large weighting factor (f) in the measured Doppler effect.

No correction to zero wall and sample thickness is warranted for the small Doppler effect in U235 fission for which the random errors dominate.

Table 3: Activation Doppler effect in U238 capture

Core No.	Temperature range	Doppler effect $D_x(\sigma_b = \infty)$
5	343 - 1780 °K	0.260 ± 0.018
	308 - 873 °K	0.151 ± 0.011
8	345 - 1750 °K	0.098 ± 0.006
3	325 - 1780 °K	0.030 ± 0.003

Table 4: Activation Doppler effect in U235 fission

Core No.	Temperature range	Doppler effect, D
5	308- 873 °K	0.004 ± 0.002
	320-1470 °K	0.007 ± 0.003
8	325-1470 °K	0.000 ± 0.002

8.2 Final results

The final results are given in Tables 3 and 4 and Figures 9-11. The errors quoted in the tables are the estimated standard deviations including random errors and uncertainties in extrapolations as discussed in the preceding paragraph.

Since the Doppler coefficient is expected to vary approximately as T^{-1} in fast reactor spectra, it is convenient to use the quantity $\log \frac{T}{T_o}$ as abscissa in a diagram of the Doppler effect versus temperature. A straight line in the diagram then represents a T^{-1} behaviour of the Doppler coefficient; a positive second derivative indicates a $T^{-\alpha}$ dependence with $\alpha < 1$, and a negative second derivative corresponds to $\alpha > 1$. The results are presented in this manner in Figures 9 (U238 capture) and 10 (U235 fission). The temperature dependence of the Doppler effect was studied only in the case of U238 and in the softest spectrum. Figure 9 indicates that the α-value is slightly smaller than 1; the value estimated by at least squares fit is $\alpha = 0.80 \pm 0.13$.

The results for U235 are illustrated in Figure 10. The Doppler effect in in U235 fission is very small in comparison with that in U238 capture. In the harder spectrum of core 8 the U235 Doppler effect is equal to zero within the experimental uncertainty of 0.2 %. In the still harder spectrum of core 3 the measurements were therefore limited to U238.

The dependence of the Doppler effect in U238 on the neutron spectrum is illustrated qualitatively in Figure 11, in which the Doppler effect is plotted versus the calculated number of U238 captures below 9.1 keV in the three assemblies. The Doppler effect is roughly proportional to this number in the studied cores.

ACKNOWLEDGEMENTS

The encouragement and useful criticism given throughout this work by Dr. E. Hellstrand is gratefully acknowledged.

Much advice and help was given by several branches of the company. We have been effectively assisted by the Numerical Group (RFN), particularly as regards coding work by Å. Ahlin and computer communications by Mrs. Karin Klingfeldt. The uranium oxide samples were manufactured at the Reactor Materials (RMB) and the Plutonium Chemistry (RKP) Sections by L. Storm and K. E. Jansson. We also wish to acknowledge the following contributions: computer calculations by R. Håkansson, construction of sample changer and design of electronics by S. Sjööquist, experimental assistance by Å. Klingfeldt, reactor operations by the FR0 and R2-0 Groups and typing of manuscript by Mrs. Paula Granath.

REFERENCES

1. STORRER F, KHAIRALLAH A and OZEROFF J,
Measurements of the Doppler Coefficient in Large Fast Power Reactors using a Fast Critical Assembly and an Experimental Fast Reactor. Proceedings of the Conference on Breeding, Economics and Safety in Large Fast Power Reactors, October 7-10, 1963. (ANL-6792, p. 823).

2. PFLASTERER Jr. G R and SHER R,
Activation Measurement of the Doppler Effect for 238 U Capture and 235 U Fission in a Fast-Neutron Spectrum.
Nucl. Sci. & Eng., 30 (1967) 374.

3. DAVEY W G and AMUNDSON P I,
Activation Measurements of the Doppler Effect in 238 U in ZPR-3 Assembly 47 (SEFOR). Trans. Am. Nucl. Soc., 9 (1966) 226.

4. SMITH M J and STEVENSON J M,
Unpublished (1967).

5. ABAGYAN L P et al.,
Investigation of Doppler effect in U-238 in the oxide blanket of the BR-1 reactor. I.A.E.A Symposium on Fast Reactor Physics and Related Safety Problems, Karlsruhe, Fed. Rep. of Germany, 30 Oct. -3 Nov. 1967. (SM-101/63).

6. PERKIN J L et al.,
Measurements and calculations of the Doppler effect on the reactions 238 U (n,γ) 235 U (n,f) and 239 Pu (n,f) with neutrons in the energy range 0-25 keV. J. Nucl. Energy. (Parts A/B Reactor Sci. Technol.) 20 (1966) 921.

7. SEUFERT H and STEGEMANN D,
Energy- and temperaturedependent capture measurements below 30 keV supporting Doppler effect calculations. 1967. Ref. 5, (SM-101/17).

8. TIRÉN L I et al.,
Studies of the Doppler Coefficient and the Reactivity Effect of Polythene in Some Fast Reactor Spectra. 1967. Ref. 5, (SM-101/3).

9. ANDERSSON T L et al.,
Experimental and Theoretical Work at the Zero Energy Fast Reactor FR0. Proceedings of the International Conference on Fast Critical Experiments and their Analysis, October 10-13, 1966. (ANL-7320, p. 159).

10. HUMMEL H H, HWANG R N and PHILLIPS K,
Recent Investigations of Fast Reactor Reactivity Coefficients. Proceedings of the Conference on Safety, Fuels and Core Design in Large Fast Power Reactors, Oct. 11-14, 1965. (ANL-7120, p. 413).

11. AHLIN Å et al.,
Accurate comparisons of the gamma-activity in irradiated uranium foils. 1967. AB Atomenergi, Sweden (Internal report TPM-FFX-70).

12. TIRÉN L I,
Studies of the Ratio of U238 Capture and U235 Fission Cross Sections in the Fast Reactor FR0.
Nukleonik 10 (1967) 141.

13. ZIMEN K E and DAHL L,
Die Diffusion von Spaltungs-Xenon aus Uranmetall. Z. Naturforsch. 12 A (1957), 167.

14. BELLE J, (ed.)
Uranium Dioxide: Properties and Nuclear Applications. Washington, USAEC, 1961.

15. Reactor physics constants. 1963. (ANL-5800. 2:nd ed., p. 281).

16. REYNOLDS A B,
Resonance Integral for the Doppler Measurement in Fast Reactors by the Foil-Activation Technique. Nucl. Sci. & Eng., 22 (1965) 487.

17. TIRÉN L I,
Resonance absorption in a lump surrounded by a homogeneous medium containing the same resonance absorber. 1967. AB Atomenergi, Sweden (Internal report TPM-FFX-84).

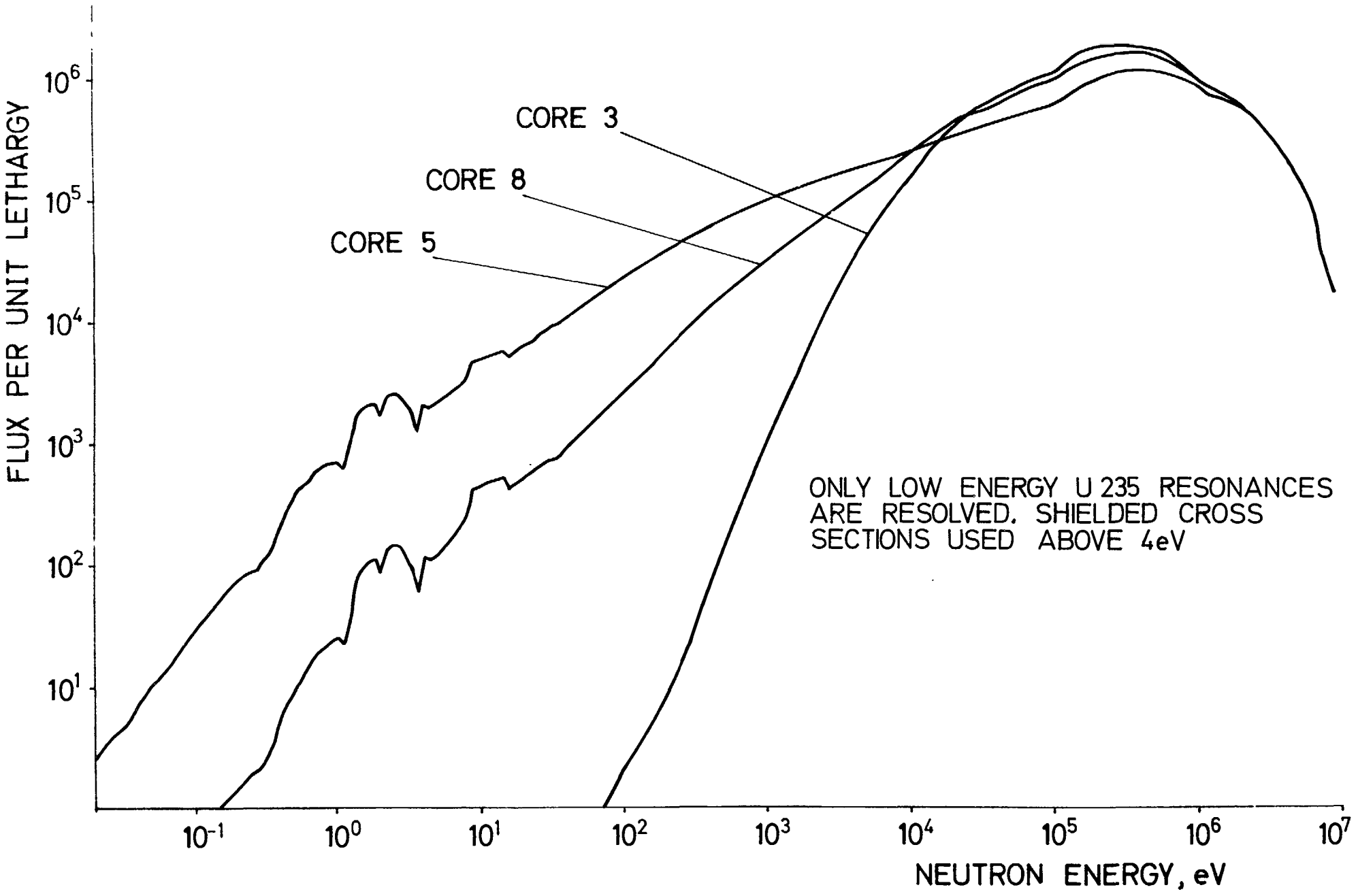

FIGURE 1: CALCULATED CORE CENTRE NEUTRON SPECTRA

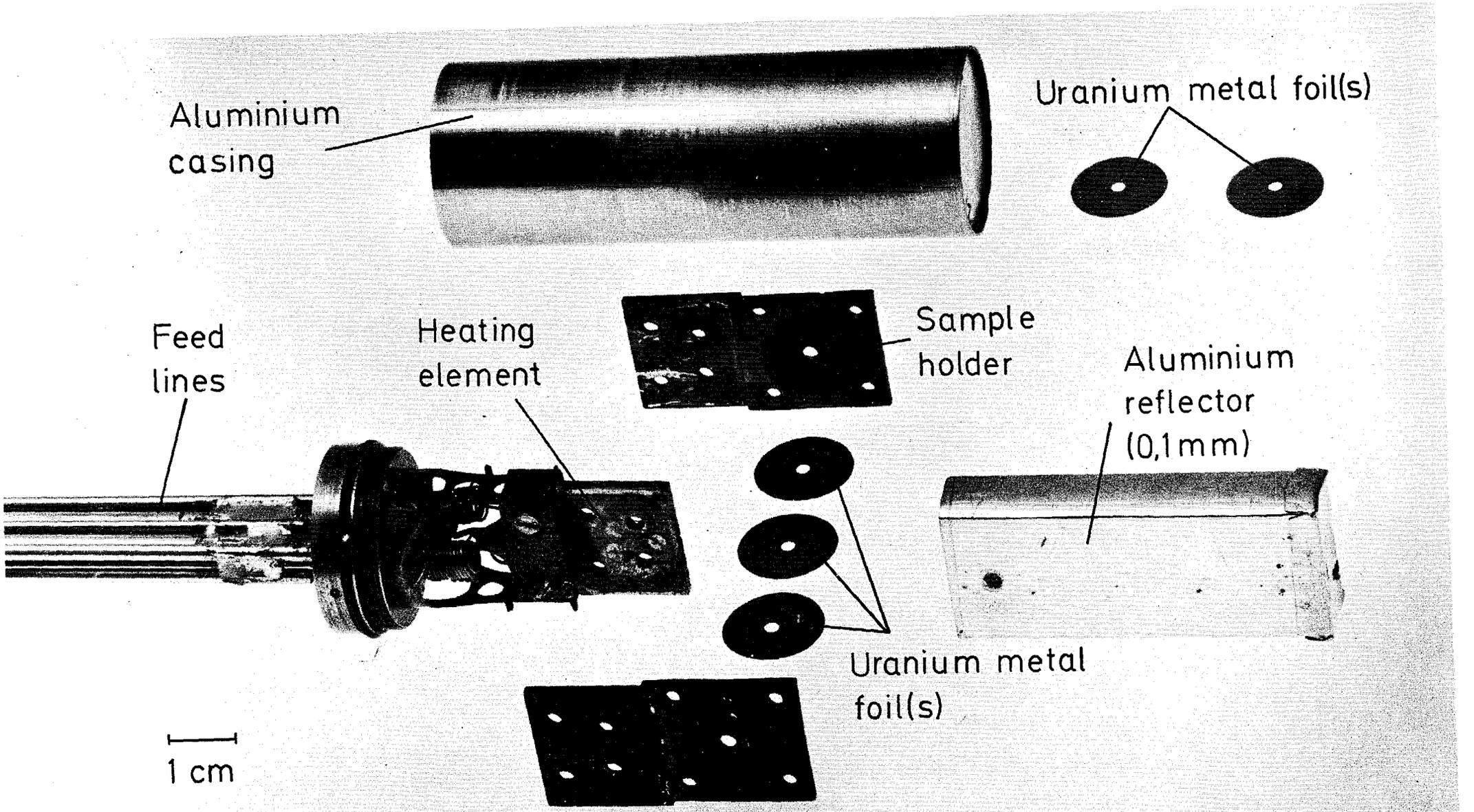

Fig. 2. Oven for heating of U-metal foils to 900° K.

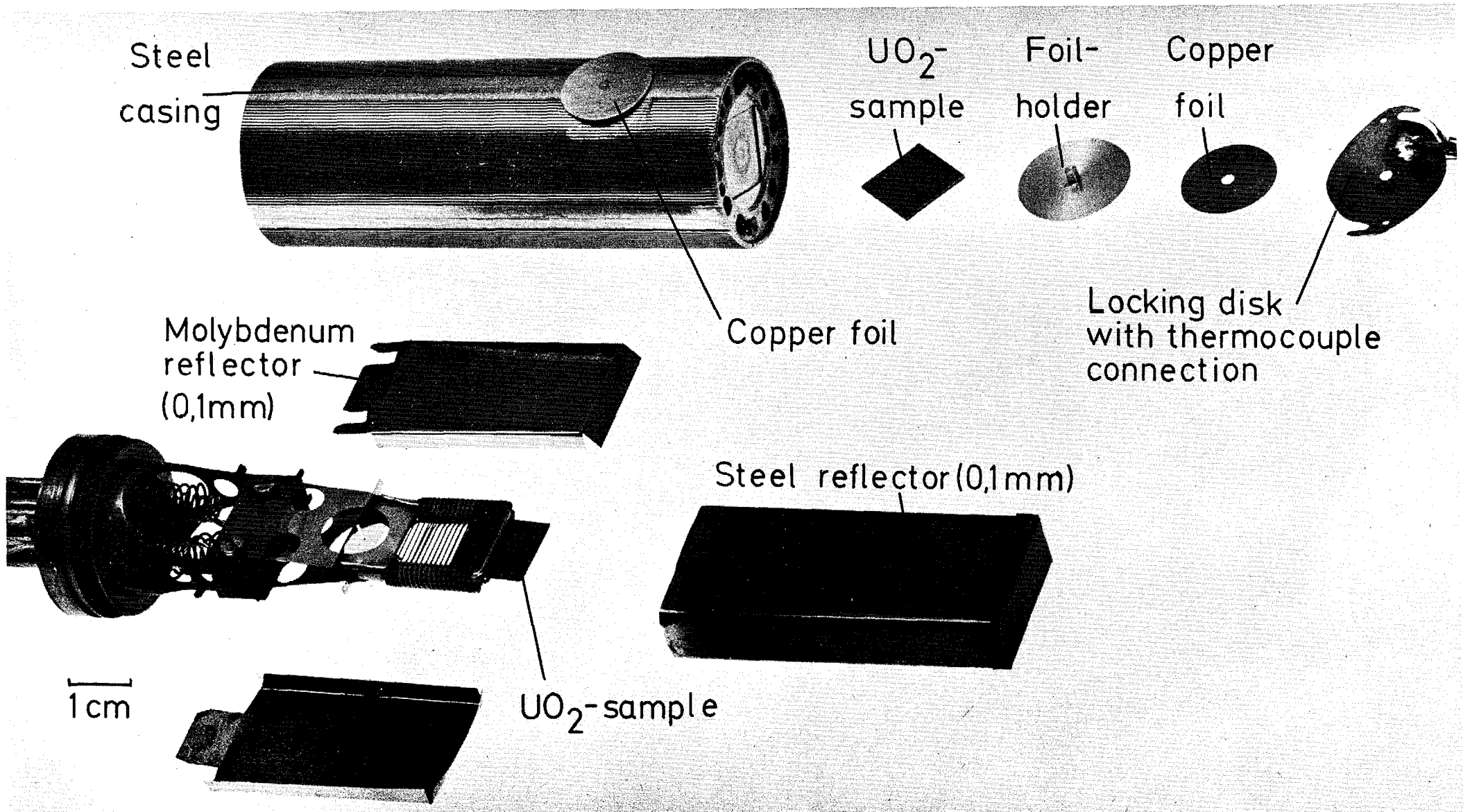

Fig. 3. Oven for heating of UO_2-plates to 1800°K.

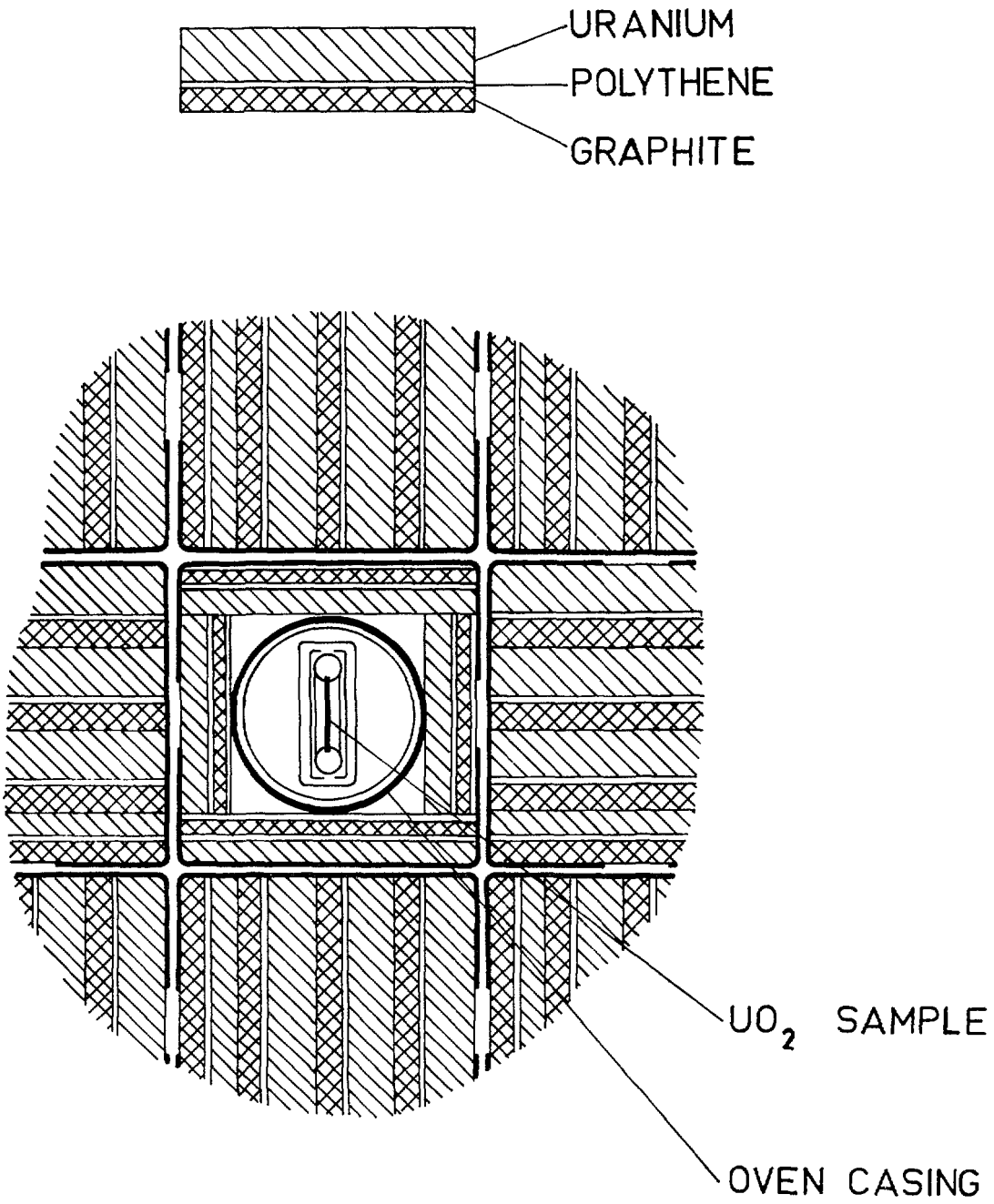

FIGURE 4: POSITIONING OF OVEN IN A FUEL ELEMENT (HETEROGENEOUS CORE 5)

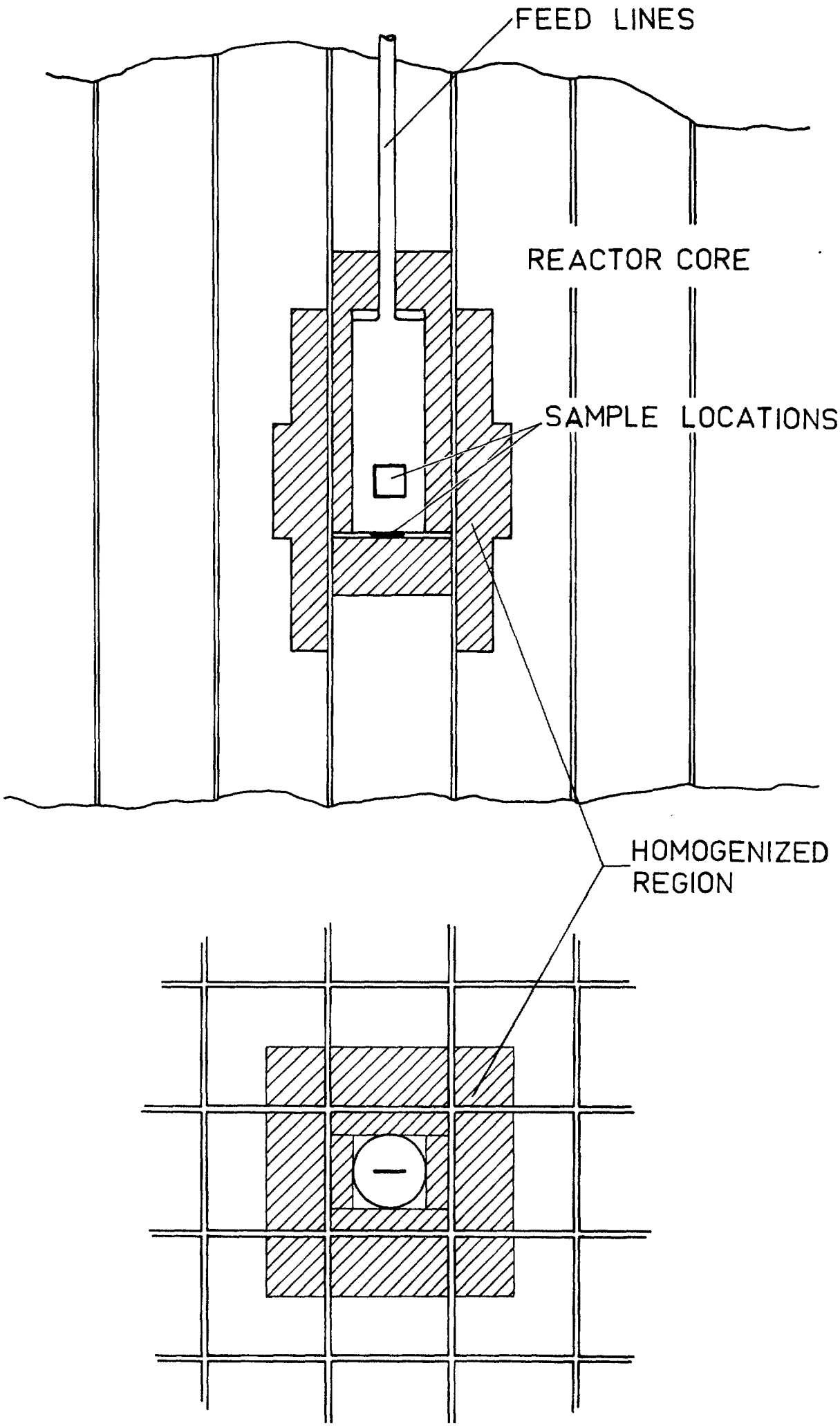

FIGURE 5: IRRADIATION ARRANGEMENT WITH HOMOGENIZED ZONE

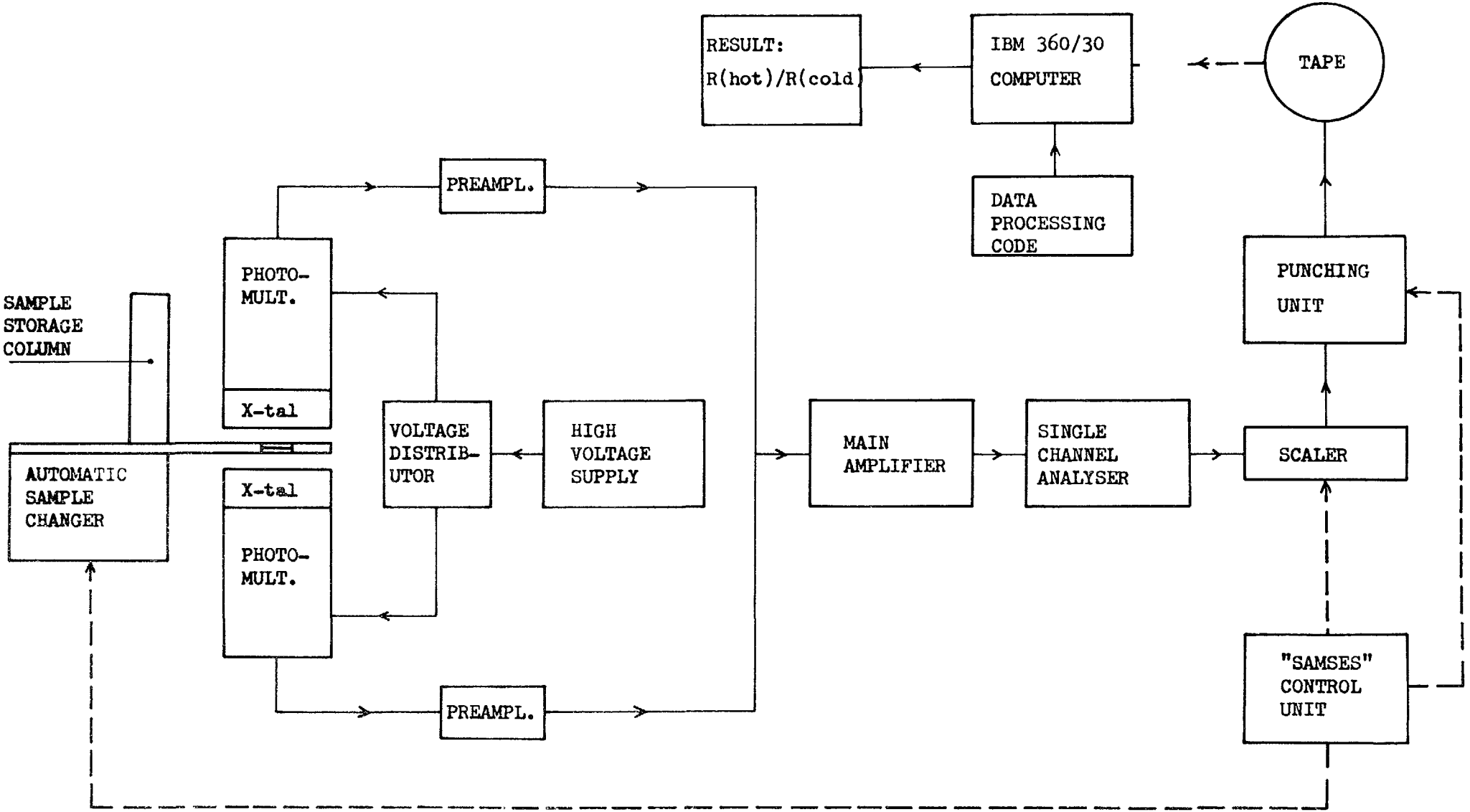

FIGURE 6: GAMMA COUNTING SYSTEM

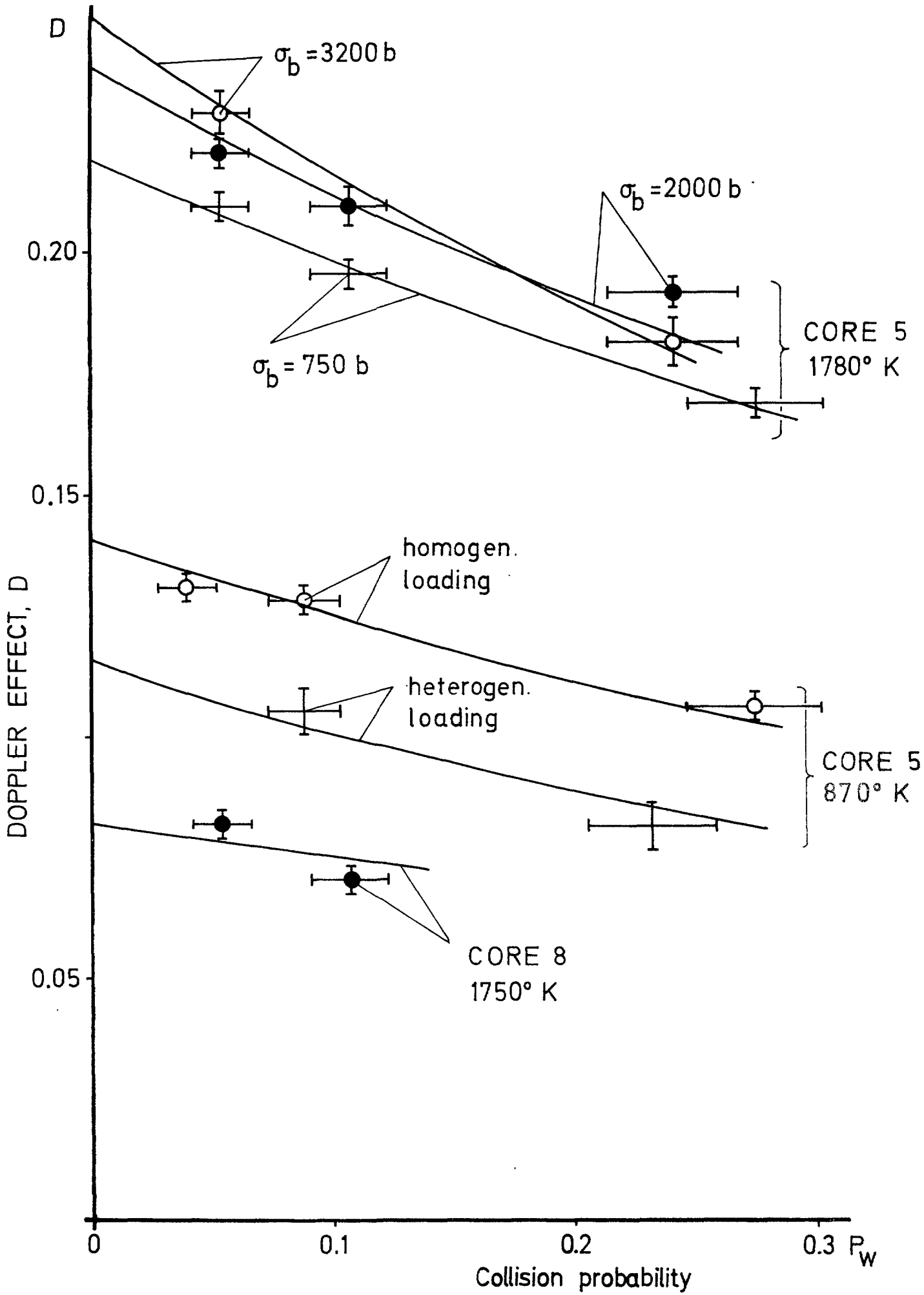

FIGURE 7: VARIATIONS IN THE DOPPLER EFFECT WITH WALL THICKNESS OF OVEN (U 238)

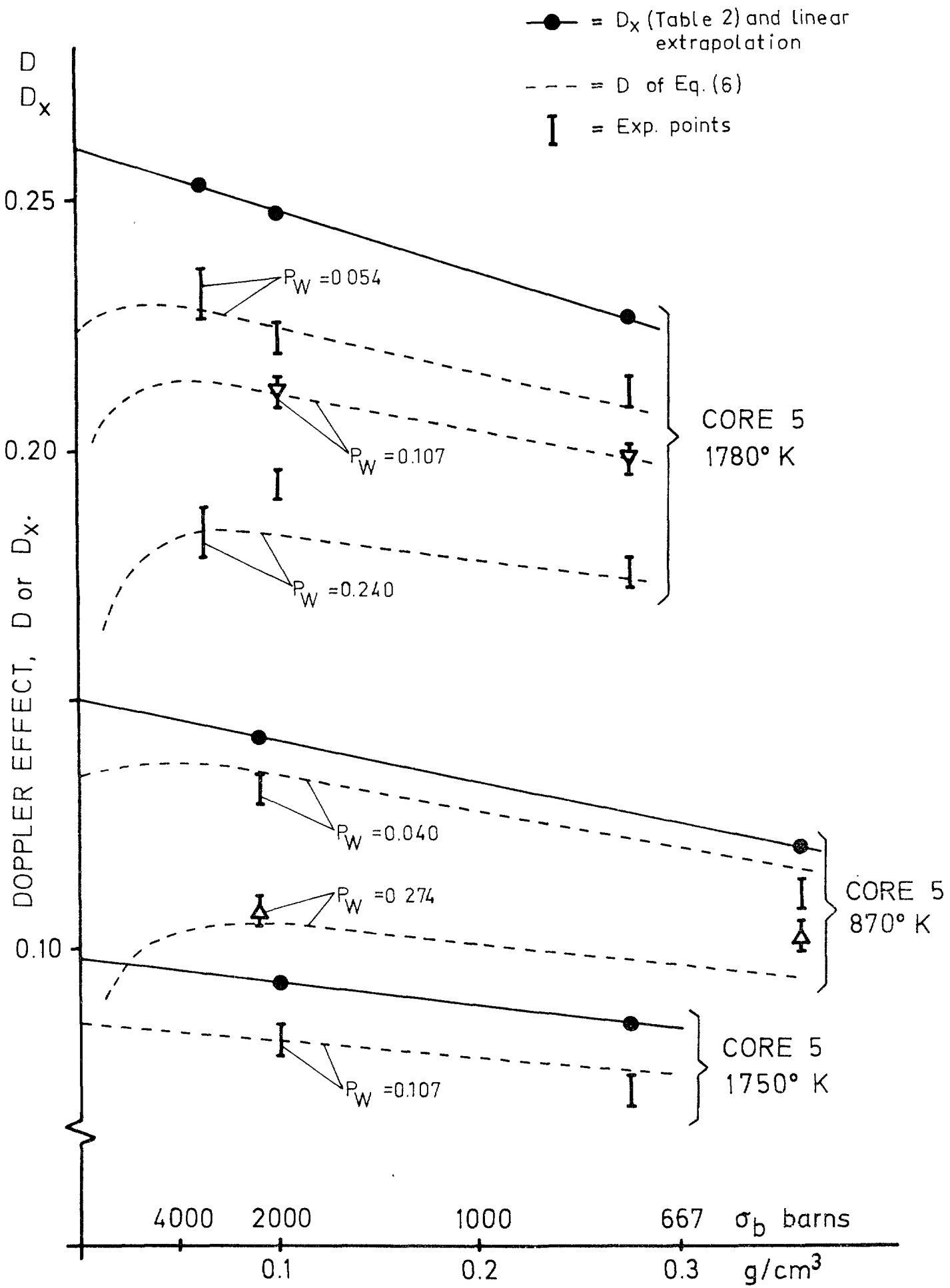

FIGURE 8: VARIATIONS IN THE DOPPLER EFFECT WITH SAMPLE THICKNESS (U 238)

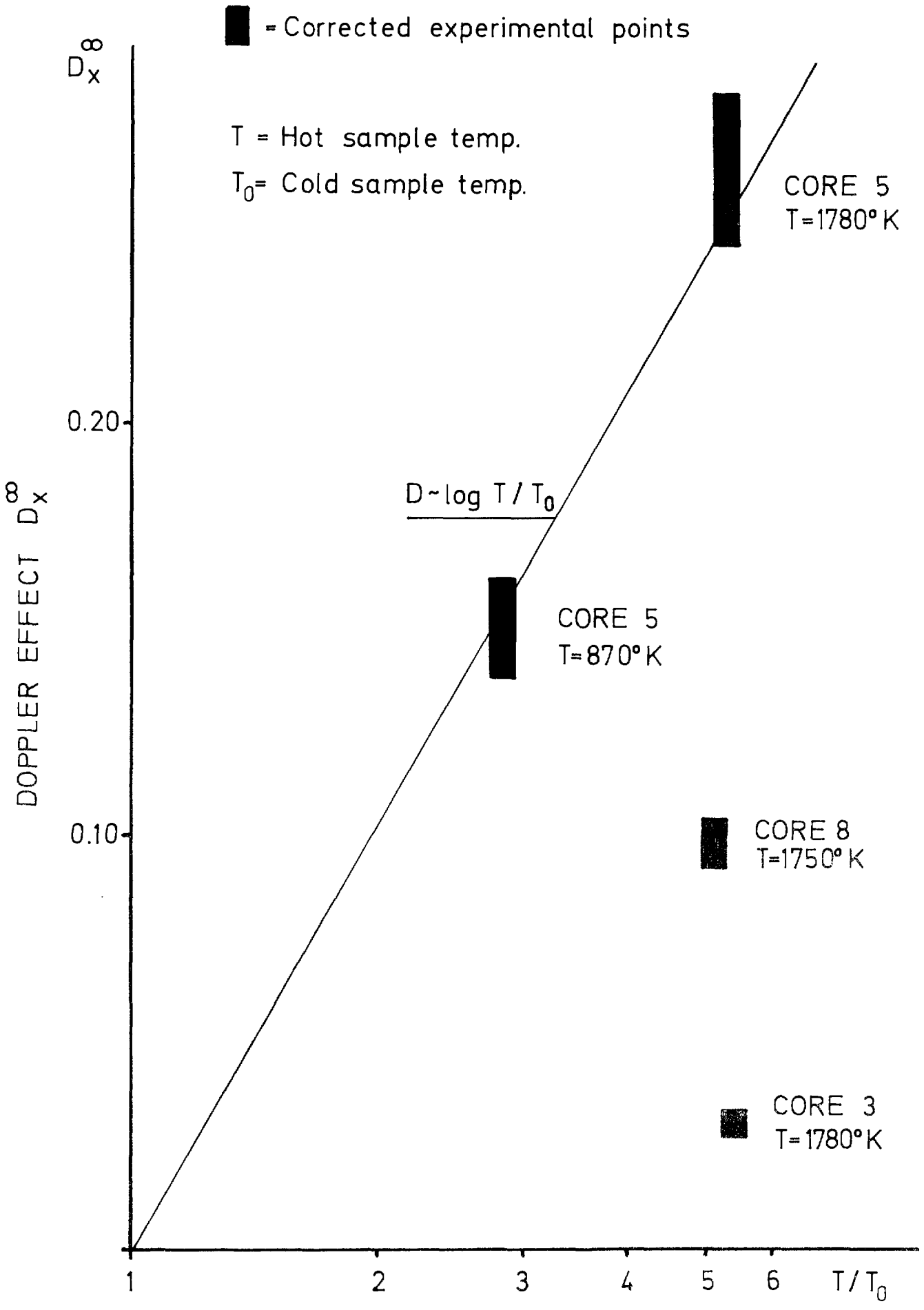

FIGURE 9: DOPPLER EFFECT IN U 238 (ZERO WALL THICKNESS AND ZERO SAMPLE THICKNESS)

Experimental points

T = Hot sample temp.

T_0 = Cold sample temp.

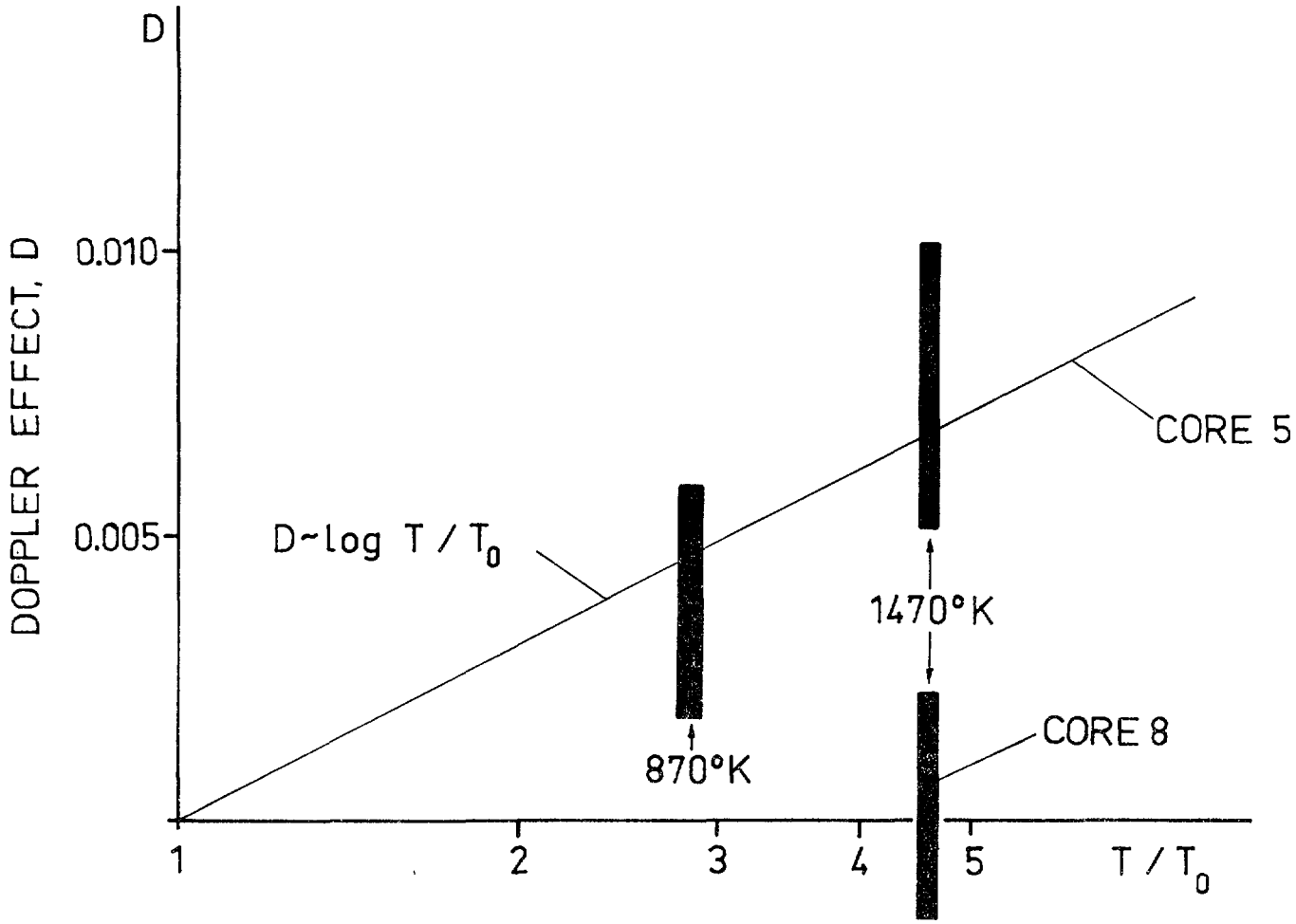

FIGURE 10: DOPPLER EFFECT IN U 235

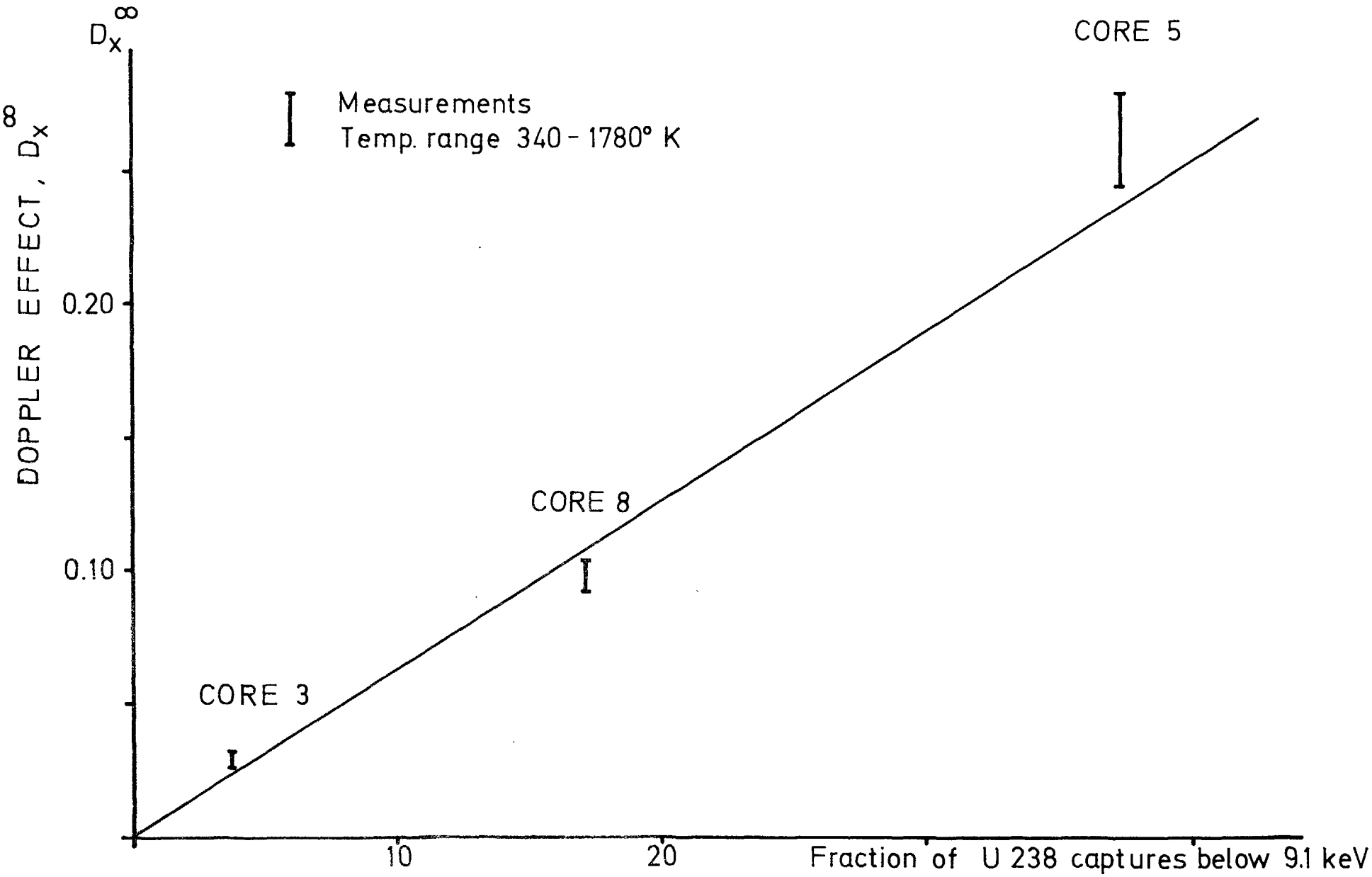

FIGURE 11: SPECTRUM DEPENDENCE OF THE DOPPLER EFFECT IN U 238

APPENDIX I

Estimate of background cross section (σ_b) in resonance cross section calculations.

In a homogeneous medium the σ_b-value associated with resonance shielding in an absorber R, is defined here as

$$\sigma_b(\text{Homogen.}) = \frac{1}{N_R} \sum_{i \neq R} N_i \sigma_i$$

The N_i:s are atomic densities of the isotopes of the medium, and σ_i is the total non-resonant cross section of isotope i.

The σ_b-concept can be extended to a heterogeneous medium by the use of equivalence theory. The expression obtained from Ref. [10] is:

$$\sigma_b = \frac{1}{N_R} \sum_{i \neq R}^{\text{"fuel"}} N_i \sigma_i + \frac{\omega}{N_R \cdot \bar{\ell}} \frac{a(1-C)}{1+(a-1)C}$$

It is assumed here that R is a constituent of a fuel pin or plate. The sum on the right side of this expression is to be taken over isotopes in the fuel only.

ω = fuel volume fraction

$\bar{\ell}$ = mean chord length of fuel lump

a = Bell factor

C = Dancoff factor

In a regular slab lattice with fuel plate thickness $t = \frac{1}{2} \bar{\ell}$ and lattice constant $d = \frac{t}{\omega}$ one obtains [15]:

$$C = 2E_3(x)$$

$$x = d \cdot \sum_{i \neq \text{fuel}} N_i \sigma_i = d \cdot N_R \sigma_{ex}$$

$$E_3(x) = \int_1^{\infty} \frac{e^{-xt}}{t^{-3}}\, dt$$

For small values of x $E_3(x)$ can be expanded in Taylor series:

$$E_3(x) = \frac{1}{2} - x + \frac{x^2}{2}\left(\frac{3}{2} - \gamma - \ln x\right) + \frac{x^3}{6} + \ldots$$

(γ = Euler's constant = 0.57721...)

In this case σ_b can be approximated by:

$$\sigma_b = \sigma_b(\text{Homogen.}) - \sigma_{ex} \cdot x\left[0.461 - \frac{1}{2}\ln x - \frac{2(a-1)}{a}\right] + \ldots$$

The above formulae have been used to estimate σ_b-values for the case of R = U238 in FR0 core 5, using a = 1.35 and the following approximate data:

Isotope	σ_i, barns
U238	-
U235	20
C12	4
H1	20
SS	8

One obtains:

σ_b(Homogen.) = 19.2 b

σ_b(t = 0.06, d = 0.13 cm) = 18.4 b

σ_b(t = 0.71, d = 1.16 cm) = 15.4 b

APPENDIX II

Estimate of the change in flux depression in a U235 disk due to thermal expansion.

The ratio of the mean value of the neutron flux in a thin foil and the flux at the foil surface is given by the formula (ANL-5800, 2:nd Ed. (1963), p. 669)

$$G(\tau) = \frac{1}{\tau}\left[\frac{1}{2} - E_3(\tau)\right]$$

$$\tau = \Sigma_a t$$

$$E_3(\tau) = \int_1^\infty \frac{e^{-\tau x}}{x^3}\,dx$$

Σ_a = macroscopic absorption cross section of foil material

t = foil thickness

Two U235 foils are compared, each of which is irradiated in a cavity (oven), one at room temperature (293 ^{o}K) and one at an elevated temperature (1473 ^{o}K). One can assume that the flux at the foil surfaces is equal. The activation ratio R(hot)/R(cold) is then

$$\frac{R(hot)}{R(cold)} = \frac{G[\tau(1473^{o})]}{G[\tau(293^{o})]}$$

or, for a small change

$$\frac{R(hot)}{R(cold)} - 1 = \frac{\Delta G(\tau)}{G(\tau)}$$

$$\Delta G(\tau) = \frac{dG}{d\tau} \cdot \frac{d\tau}{dT} \cdot \Delta T$$

where ΔT is the temperature change.

One obtains, since τ is inversely proportional to the foil area, S:

$$\Delta G(\tau) = -\tau \cdot \frac{dG}{d\tau} \cdot \left(\frac{1}{S}\frac{dS}{dT}\right) \cdot \Delta T$$

$\frac{1}{S}\frac{dS}{dT} = 2\alpha$, α being the linear thermal expansion coefficient.

The following data are valid for our 0.3 mm U235 oxide disks (93 % U235):

$m = 0.45$ g (foil weight)

$S = 1.44\ cm^2$

$\sigma_a = 614$ barns

$\tau = 0.403$

$G = 0.610$

$(\frac{dG}{d\tau})_{0.4} = -0.550$

The linear expansion $\alpha\Delta T$ is given by the following formula, which was obtained for UO_2 manufactured by a procedure similar to that of our samples (J. B. Conway et al.: The Thermal Expansion and Heat Capacity of UO_2 to 2200 °C, Trans. Am. Nucl. Soc. 6, 153 (1963)):-

$$\alpha\Delta T(\%) = 1.732\times10^{-2}+6.797\times10^{-4}T+2.896\times10^{-7}T^2$$

in the temperature range T = 1000° to 2000 °C. With T = 1200 °C the numerical value is $\underline{\alpha\Delta T = 0.0125}$.

One then obtains

$$\frac{R(hot)}{R(cold)} - 1 = 0.0091$$

This value has been used to correct for the effect of thermal expansion in Section 7.2.

LIST OF PUBLISHED AE-REPORTS

1–240. (See the back cover earlier reports.)

241. Burn-up determination by high resolution gamma spectrometry: spectra from slightly-irradiated uranium and plutonium between 400–830 keV. By R. S. Forsyth and N. Ronqvist. 1966. 22 p. Sw. cr. 8:–.

242. Half life measurements in ^{155}Gd. By S. G. Malmskog. 1966. 10 p. Sw. cr. 8:–.

243. On shear stress distributions for flow in smooth or partially rough annuli. By B. Kjellström and S. Hedberg. 1966. 66 p. Sw. cr. 8:–.

244. Physics experiments at the Ågesta power station. By G. Apelqvist, P.-A. Bliselius, P. E. Blomberg, E. Jonsson and F. Åkerhielm. 1966. 30 p. Sw. cr. 8:–.

245. Intercrystalline stress corrosion cracking of inconel 600 inspection tubes in the Ågesta reactor. By B. Grönwall, L. Ljungberg, W. Hübner and W. Stuart. 1966. 26 p. Sw. cr. 8:–.

246. Operating experience at the Ågesta nuclear power station. By S. Sandström. 1966. 113 p. Sw. cr. 8:–.

247. Neutron-activation analysis of biological material with high radiation levels. By K. Samsahl. 1966. 15 p. Sw. cr. 8:–.

248. One-group perturbation theory applied to measurements with void. By R. Persson. 1966. 19 p. Sw. cr. 8:–.

249. Optimal linear filters. 2. Pulse time measurements in the presence of noise. By K. Nygaard. 1966. 9 p. Sw. cr. 8:–.

250. The interaction between control rods as estimated by second-order one-group perturbation theory. By R. Persson. 1966. 42 p. Sw. cr. 8:–.

251. Absolute transition probabilities from the 453.1 keV level in 183W. By S. G. Malmskog. 1966. 12 p. Sw. cr. 8:–.

252. Nomogram for determining shield thickness for point and line sources of gamma rays. By C. Jönemalm and K. Malén. 1966. 33 p. Sw. cr. 8:–.

253. Report on the personnel dosimetry at AB Atomenergi during 1965. By K. A. Edwardsson. 1966. 13 p. Sw. cr. 8:–.

254. Buckling measurements up to 250°C on lattices of Ågesta clusters and on D_2O alone in the pressurized exponential assembly TZ. By R. Persson, A. J. W. Andersson and C-E. Wikdahl. 1966. 56 p. Sw. cr. 8:–.

255. Decontamination experiments on intact pig skin contaminated with beta-gamma-emitting nuclides. By K. A. Edwardsson, S. Hagsgård and Å. Swensson. 1966. 35 p. Sw. cr. 8:–.

256. Perturbation method of analysis applied to substitution measurements of buckling. By R. Persson. 1966. 57 p. Sw. cr. 8:–.

257. The Dancoff correction in square and hexagonal lattices. By I. Carlvik. 1966 35 p. Sw. cr. 8:–.

258. Hall effect influence on a highly conducting fluid. By E. A. Witalis. 1966. 13 p. Sw. cr. 8:–.

259. Analysis of the quasi-elastic scattering of neutrons in hydrogenous liquids. By S. N. Purohit. 1966. 26 p. Sw. cr. 8:–.

260. High temperature tensile properties of unirradiated and neutron irradiated 20Cr–35Ni austenitic steel. By R. B. Roy and B. Solly. 1966. 25 p. Sw. cr. 8:–.

261. On the attenuation of neutrons and photos in a duct filled with a helical plug. By E. Aalto and Å. Krell. 1966. 24 p. Sw. cr. 8:–.

262. Design and analysis of the power control system of the fast zero energy reactor FR-0. By N. J. H. Schuch. 1966. 70 p. Sw. cr. 8:–.

263. Possible deformed states in ^{115}In and ^{117}In. By A. Bäcklin, B. Fogelberg and S. G. Malmskog. 1967. 39 p. Sw. cr. 10:–.

264. Decay of the 16.3 min. ^{182}Ta isomer. By M. Höjeberg and S. G. Malmskog. 1967. 13 p. Sw. cr. 10:–.

265. Decay properties of ^{147}Nd. By A. Bäcklin and S. G. Malmskog. 1967. 15 p. Sw. cr. 10:–.

266. The half life of the 53 keV level in ^{197}Pt. By S. G. Malmskog. 1967. 10 p. Sw. cr. 10:–.

267. Burn-up determination by high resolution gamma spectrometry: Axial and diametral scanning experiments. By R. S. Forsyth, W. H. Blackladder and N. Ronqvist. 1967. 18 p. Sw. cr. 10:–.

268. On the properties of the $s_{1/2} \longrightarrow d_{3/2}$ transition in ^{199}Au. By A. Bäcklin and S. G. Malmskog. 1967. 23 p. Sw. cr. 10:–.

269. Experimental equipment for physics studies in the Ågesta reactor. By G. Bernander, P. E. Blomberg and P.-O. Dubois. 1967. 35 p. Sw. cr. 10:–.

270. An optical model study of neutrons elastically scattered by iron, nickel, cobalt, copper, and indium in the energy region 1.5 to 7.0 MeV. By B. Holmqvist and T. Wiedling. 1967. 20 p. Sw. cr. 10:–.

271. Improvement of reactor fuel element heat transfer by surface roughness. By B. Kjellström and A. E. Larsson. 1967. 94 p. Sw. cr. 10:–.

272. Burn-up determination by high resolution gamma spectrometry: Fission product migration studies. By R. S. Forsyth, W. H. Blackadder and N. Ronqvist. 1967. 19 p. Sw. cr. 10:–.

273. Monoenergetic critical parameters and decay constants for small spheres and thin slabs. By I. Carlvik. 1967. 24 p. Sw. cr. 10:–.

274. Scattering of neutrons by an anharmonic crystal. By T. Högberg, L. Bohlin and I. Ebbsjö. 1967. 38 p. Sw. cr. 10:–.

275. The $|\Delta K| = 1$, E1 transitions in odd-A isotopes of Tb and Eu. By S. G. Malmskog, A. Marelius and S. Wahlborn. 1967. 24 p. Sw. cr. 10:–.

276. A burnout correlation for flow of boiling water in vertical rod bundles. By Kurt M. Becker. 1967. 102 p. Sw. cr. 10:–.

277. Epithermal and thermal spectrum indices in heavy water lattices. By E. K. Sokolowski and A. Jonsson. 1967. 44 p. Sw. cr. 10:–.

278. On the $d_{5/2} \leftrightarrow g_{7/2}$ transitions in odd mass Pm nuclei. By A. Bäcklin and S. G. Malmskog. 1967. 14 p. Sw. cr. 10:–.

279. Calculations of neutron flux distributions by means of integral transport methods. By I. Carlvik. 1967. 94 p. Sw. cr. 10:–.

280. On the magnetic properties of the K=1 rotational band in ^{188}Re. By S. G. Malmskog and M. Höjeberg. 1967. 18 p. Sw. cr. 10:–.

281. Collision probabilities for finite cylinders and cuboids. By I. Carlvik. 1967. 28 p. Sw. cr. 10:–.

282. Polarized elastic fast-neutron scattering of ^{12}C in the lower MeV-range. I. Experimental part. By O. Aspelund. 1967. 50 p. Sw. cr. 10:–.

283. Progress report 1966. Nuclear chemistry. 1967. 26 p. Sw. cr. 10:–.

284. Finite-geometry and polarized multiple-scattering corrections of experimental fast-neutron polarization data by means of Monte Carlo methods. By O. Aspelund and B. Gustafsson. 1967. 60 p. Sw. cr. 10:–.

285. Power disturbances close to hydrodynamic instability in natural circulation two-phase flow. By R. P. Mathisen and O. Eklind. 1967. 34 p. Sw. cr. 10:–.

286. Calculation of steam volume fraction in subcooled boiling. By S. Z. Rouhani. 1967. 26. p. Sw. cr. 10:–.

287. Absolute E1, $\Delta K = 0$ transition rates in odd-mass Pm and Eu-isotopes. By S. G. Malmskog. 1967. 33 p. Sw. cr. 10:–.

288. Irradiation effects in Fortiweld steel containing different boron isotopes. By M. Grounes. 1967. 21 p. Sw. cr. 10. .

289. Measurements of the reactivity properties of the Ågesta nuclear power reactor at zero power. By G. Bernander. 1967. 43 p. Sw. cr. 10:–.

290. Determination of mercury in aqueous samples by means of neutron activation analysis with an account of flux disturbances. By D. Brune and K. Jirlow. 1967. 15 p. Sw. cr. 10:–.

291. Separtaion of ^{51}Cr by means of the Szilard-Chalmers effect from potassium chromate irradiated at low temperature. By D. Brune. 1967. 15 p. Sw. cr. 10:–.

292. Total and differential efficiencies for a circular detector viewing a circular radiator of finite thickness. By A. Lauber and B. Tollander. 1967. 45 p. Sw. cr. 10:–.

293. Absolute M1 and E2 transition probabilities in ^{233}U. By S. G. Malmskog and M. Höjeberg. 1967. 37 p. Sw. cr. 10:–.

294. Cerenkov detectors for fission product monitoring in reactor coolant water. By O. Strindehag. 1967. 56 p. Sw. cr. 10:–.

295. RPC calculations for K-forbidden transitions in ^{183}W. Evidence for large inertial parameter connected with high-lying rotational bands. By S. G. Malmskog and S. Wahlborn. 1967. 25 p. Sw. cr. 10:–.

296. An investigation of trace elements in marine and lacustrine deposits by means of a neutron activation method. By O. Landström, K. Samsahl and C-G. Wenner. 1967. 40 p. Sw. cr. 10:–.

297. Natural circulation with boiling. By R. P. Mathisen. 1967. 58 p. Sw. cr. 10:–.

298. Irradiation effects at 160–240°C in some Swedish pressure vessel steels. By M. Grounes, H. P. Myers and N-E. Hannerz. 1967. 36 p. Sw. cr. 10:–.

299. The measurement of epithermal-to-thermal U-238 neutron capture rate (ρ_{28}) in Ågesta power reactor fuel. By G. Bernander. 1967. 42 p. Sw. cr. 10:–.

300. Levels and transition rates in ^{199}Au. By S. G. Malmskog, A. Bäcklin and B. Fogelberg. 1967. 48 p. Sw. cr. 10:–.

301. The present status of the half-life measuring equipment and technique at Studsvik. By S. G. Malmskog. 1967. 26 p. Sw. cr. 10:–.

302. Determination of oxygen in aluminum by means of 14 MeV neutrons with an account of flux attenuation in the sample. By D. Brune and K. Jirlow. 1967. 16 p. Sw. cr. 10:–.

303. Neutron elastic scattering cross sections of the elements Ni, Co, and Cu between 1.5 and 8.0 mev. By B. Holmqvist and T. Wiedling. 1967. 17 p. Sw. cr. 10:–.

304. A study of the energy dependence of the Th232 capture cross section in the energy region 0.1 to 3.4 eV. By G. Lundgren. 1967. 25 p. Sw. cr. 10:–.

305. Studies of the reactivity effect of polythene in the fast reactor FRO. By L. I. Tirén and R. Håkansson. 1967. 25 p. Sw. cr. 10:–.

306. Final report on IFA-10, the first swedish instrumented fuel assembly irradiated in HBWR, Norway. By J-Å. Gyllander. 1967. 35 p. Sw. cr. 10:–.

307. Solution of large systems of linear equations with quadratic or non-quadratic matrices and deconvolution of spectra. By K. Nygaard. 1967. 15 p. Sw. cr. 10:–.

308. Irradiation of superheater test fuel elements in the steam loop of the R2 reactor. By F. Ravndal. 1967. 94 p. Sw. cr. 10:–.

309. Measurement of the decay of thermal neutrons in water poisoned with the non-1/v neutron absorber cadium. By L. G. Larsson and E. Möller. 1967. 20 p. Sw. cr. 10:–.

310. Calculated absolute detection efficiencies of cylindrical NaI (Tl) scintillation crystals for aqueous spherical sources. By. O. Strindehag and B. Tollander. 1968. 18 p. Sw. cr. 10:–.

311. Spectroscopic study of recombination in the early afterglow of a helium plasma. By J. Stevefelt. 1968. 49 p. Sw. cr. 10:–.

312. Report on the personnel dosimetry at AB Atomenergi during 1966. By J. Carlsson and T. Wahlberg. 1968. 10 p. Sw. cr. 10:–.

313. The electron temperature of a partially ionized gas in an electric field. By F. Robben. 1968. 16 p. Sw. cr. 10:–.

314. Activation Doppler measurements on U238 and U235 in some fast reactor spectra. By L. I. Tirén and I. Gustafsson. 1968. 40 p. Sw. cr. 10:–.

Förteckning över publicerade AES-rapporter

1. Analys medelst gamma-spektrometri. Av D. Brune. 1961. 10 s. Kr 6:–.
2. Bestrålningsförändringar och neutronatmosfär i reaktortrycktankar – några synpunkter. Av M. Grounes. 1962. 33 s. Kr 6:–.
3. Studium av sträckgränsen i mjukt stål. Av G. Östberg och R. Attermo 1963. 17 s. Kr 6:–.
4. Teknisk upphandling inom reaktorområdet. Av Erik Jonson. 1963. 64 s. Kr 8:–
5. Ågesta Kraftvärmeverk. Sammanställning av tekniska data, beskrivningar m. m. för reaktordelen. Av B. Lilliehöök. 1964. 336 s. Kr 15:–.
6. Atomdagen 1965. Sammanställning av föredrag och diskussioner. Av S. Sandström. 1966. 321 s. Kr 15:–.
7. Radiumhaltiga byggnadsmaterial ur strålskyddssynpunkt. Av Stig O. W. Bergström och Thor Wahlberg. 1967. 26 s. Kr 10:–.

Additional copies avaiable at the library of AB Atomenergi, Studsvik, Nyköping, Sweden. Micronegatives of the reports are obtainable through Filmprodukter, Gamla landsvägen 4, Ektorp, Sweden.

EOS-tryckerierna, Stockholm 1968